Efficacy of Self-assembled Hydrogels Composed of Positively or Negatively Charged Peptides as Scaffolds for Cell Culture

AYA NAGAYASU,[1,2] HIDENORI YOKOI,[2] JUN A. MINAGUCHI,[1] YOSHINAO Z. HOSAKA,[1,3] HIROMI UEDA[1] AND KAZUSHIGE TAKEHANA[1,*]

[1]*Department of Veterinary Anatomy, School of Veterinary Medicine, Rakuno Gakuen University, 582, Midorimachi, Bunkyodai, Ebetsu, Hokkaido 069-8501, Japan*

[2]*Menicon Co., Ltd., 5-1-10, Takamoridai, Kasugai, Aichi 478-0032, Japan*

[3]*Faculty of Agriculture, Department of Veterinary Anatomy, Tottori University, 4-101, Koyama-Minami, Tottori 680-8550, Japan*

ABSTRACT: KASEA16(+) and KASEA16(−) peptides, the net charges of which are positive and negative, respectively, under a neutral condition could undergo self-assembly into nanofibers and form transparent hydrogels without peptide aggregation upon rapid pH neutralization. The numbers of NIH3T3 cells attached to the KASEA16(+) hydrogel and KASEA16(−) hydrogel were similar, and cells proliferated with time on both hydrogels. Cells on the KASEA16(+) hydrogel had spindle-like morphology, while cells on the KASEA16(−) hydrogel formed clusters without extending cytoplasmic processes. Comparison of differently charged peptides under a neutral condition suggested that the charges of the scaffolds should be taken into consideration for the best design and selection of scaffolds for cell culture. Since the KASEA16(+) peptide could form a stable hydrogel under a neutral condition and the hydrogel served as a scaffold for cell proliferation, the KASEA16(+) hydrogel will be a useful scaffold for cell culture.

KEY WORDS: cell culture, hydrogel, peptide, scaffold, self-assembly.

*Author to whom correspondence should be addressed.
E-mail: takechan@rakuno.ac.jp
Figure 2 appears in color online: http://jba.sagepub.com

0885-3282/12/06 0651–15 $10.00/0 DOI: 10.1177/0885328210379927

INTRODUCTION

Scaffolds that mimic the extracellular matrix are a necessary component in tissue engineering, especially for cell proliferation and differentiation [1–4]. Scaffolds are typically made of high molecular weight polymers of synthetic origin such as derivatives of acrylic acids, ethylene oxides, and vinyl alcohol or from natural sources such as collagen and gelatin [5,6]. The former scaffolds such as PLLA, PLGA, PLLA–PLGA copolymers have been developed for culturing cells in three-dimensional environment. However, processed synthetic polymers consist of microfibers ~10–50 μm in diameter, similar to the size of most cells. Thus, cells attached to microfibers are still in a two-dimensional environment. Therefore, in order to culture cells in a truly three-dimensional microenvironment, the fibers must be much smaller than cells. In consequence, cells can be cultured in environment similar to extracellular matrices [7] Scaffolds obtained from natural sources have advantages over synthetic scaffolds in terms of biodegradability, biocompatibility, and cell attachment. Thus, natural scaffolds are more applicable *in vivo* [5,6]. The usefulness of atelocollagen, a weakly antigenic molecule, has already been demonstrated [8–18]. However, materials obtained from natural sources are extracted from animal tissues and have problems such as accompanying infection and physical instability. Therefore, safe and stable scaffolds to serve the requirements of biodegradability and biocompatibility are needed [1,2,6]. Recently, interest has been shown in peptides and their derivatives with self-assembling ability to form hydrogels [19–23]. For example, EAK16-II ([CH_3CO]–AEAEAKAKAEAEAKAK–[$CONH_2$]), a 16-amino-acid peptide with alternating hydrophobic and hydrophilic arrangement that corresponds to the amino acid residues 310–325 of zuotin, a Z-DNA binding protein, was discovered by Zhang et al. [24]. In aqueous solution, EAK16-II peptide undergoes self-assembly into an antiparallel β-sheet structure and forms nanofibers that further assemble into a three-dimensional meshwork structure and then hydrogel with a high water content [6,19,20,25,26]. Due to its basic structural similarities to collagen fibers, this hydrogel is considered to be a potential scaffold material for cell culture [25,26]. However, characteristics of the self-assembling peptides may vary depending on the number and types of amino acid constituents. Many EAK16-II-like peptides, for example, RADA16, EAK16-II, KLD-12, and KFE12 [4,23,26–32], have also been used as scaffold materials in culture systems for fibroblasts, chondrocytes, osteoblasts and neurons, and for promotion of tissue repair *in vivo*. However, peptide aggregation, which is not desirable for a

three-dimensional cell culture system, can occur when these hydrogels are stirred under a neutral condition. Such undesired aggregation is due to electrostatic interactions between their positively and negatively charged amino acid component residues [21,33]. The aggregate peptide shows not filament but globular pieces under an atomic force microscope [21,34]. To solve the problem of peptide aggregation, it is necessary to mix cells with an acidic aqueous solution prior to the formation of hydrogel and then gradually neutralize pH of the hydrogel–cell mixture by gradual solvent substitution [21,30,35,36]. It has been reported that the undesired aggregation of these self-assembling peptides is due to their net charge, which is zero under a neutral condition [21,33]. Consequently, it is expected that positively or negatively charged peptides under a neutral condition may self-assemble to form hydrogels with a high level of stability. In this study, a new positively charged KASEA16(+) peptide and a new negatively charged KASEA16(−) peptide were designed and their hydrogel formation ability was evaluated. The usefulness of these hydrogels as scaffolds for NIH3T3 cell culture was also investigated.

MATERIALS AND METHODS

Peptide Synthesis

Peptides, RADA16 ([CH_3CO]–RADARADARADARADA–[$CONH_2$]), KASEA16(+) ([CH_3CO]–KASAKAEAKAEAKASA–[$CONH_2$]) and KASEA16(−) ([CH_3CO]–SAEAKAEAKAEASAEA–[$CONH_2$]), were synthesized by the standard solid phase method using 9-fluorenylmethoxycarbonyl (Fmoc) chemistry on a PSSM-8 automated peptide synthesizer (Shimazu Co. Ltd., Kyoto, Japan). All peptides were prepared on CLEAR^{TM}-amide resin (Peptide Institute Inc., Osaka, Japan) in dimethylformamide (DMF) via 1-hydroxy-7-benzotriazole (HOBt)/N,N′-diisopropylcarbodiimide (DIPCI) activation. To protect the N-terminal region of each of the peptides by an acethyl group, 10 times molar weight of acetic anhydride was reacted for 2 h in DMF. Cleavage of the peptide from each solid support was performed by using a mixture of trifluoroacetic acid, 1,2-ethanedithiol, thioanisole, and water in a ratio of 190:17:10:10 for 5 h at room temperature. An excess amount of cold diethylether was added to the cleavage mixture, and the peptide was precipitated. The white precipitate was collected by centrifuging, washing with cold ether, and drying in air. The peptide powder was dissolved in Milli-Q^{TM} water (Millipore, MA, USA) and freeze-dried. Further purification was not performed.

The molecular weights of these crude peptides were measured by matrix-assisted laser desorption ionization-time of flight-mass spectroscopy (MALDI-TOF-MS).

The net charge of the peptide at each pH was calculated using the program EMBL WWW Gateway to Isoelectric Point Service (http://www.embl-heidelberg.de/cgi/pi-wrapper.pl), which is based on Lehninger's method [37]. The N- and C-terminal regions of the peptides in this study were protected, and therefore the net charge of 16-residue polyalanine in which only the terminus was charged was subtracted from the value of each peptide.

Preparation of Self-assembling Peptide Hydrogel and Atelocollagen Gel

The peptide RADA16 was dissolved in sterilized Milli-Q water (10 mg/1900 μL), and then 100 μL of 100 mM NaOH was added to the peptide solution to increase the pH value. The peptide solution with a final concentration of 0.5 wt% was added to 96-well tissue culture plates (100 μL/well) (TPP, Trasadingen, Switzerland), and the plates were placed in a humidified incubator at 37°C under 5% CO_2 to initiate peptide hydrogel formation. Gradual adjustment from acidic to neutral pH was made through a solvent substitution by adding a culture medium (Dulbecco's modified Eagle's medium; DMEM, Sigma, MO, USA) onto the peptide hydrogel (100 μL/well). This hydrogel was used for cell culture and morphological analysis. Concentrations of the peptides KASEA16(+) and KASEA16(−) were adjusted to 1.0 wt% with sterilized Milli-Q water. An equivalent amount of 100 mM HEPES buffer (pH 7.4) was added to reduce the concentration to 0.5 wt%, neutralize pH, and allow hydrogel formation. The container was inverted to confirm successful formation of non-collapsing gel [21]. For cell culture and morphological analysis, 0.5 wt% peptide solution with neutral pH was added to 96-well tissue culture plates (100 μL/well). Solvent substitution was executed after the hydrogel had formed. Since KASEA16(−) hydrogel contracted in the well (data not shown), the peptide KASEA16(−) was dissolved to 0.5 wt% with sterilized Milli-Q water and neutralized by a solvent substitution to allow gelation.

Atelocollagen gel (AG) was prepared from liquid atelocollagen solution (Koken, Tokyo, Japan) by incubation for 1 h at 37°C under 5% CO_2 in a humidified incubator. Then the gel was used for cell culture and morphological analysis.

Morphological Analysis of Self-assembling Peptide Hydrogel and AG by Scanning Electron Microscopy

Self-assembling peptide hydrogel (SPG) and AG were each processed through fixation in 3.0% glutaraldehyde in 100 mM HEPES buffer (pH 7.4) for 2 h at room temperature, post-fixation in 1.0% osmium tetroxide in 0.1 M phosphate buffer for 1 h at room temperature, washing with distilled water, and dehydration in a graded ethanol series. Thereafter, the samples were freeze-dried using t-butyl alcohol [38], mounted on metal stubs, coated with osmium using an osmium plasma coater (Nippon Laser & Electronics, Aichi, Japan), and observed by a scanning electron microscope (JSM-6000F, JEOL, Tokyo, Japan) with an accelerating voltage of 3 kV. Measurement of nanofiber diameter was performed for 30 fibers using Image J software (version 1.30) and the average diameter was calculated.

Cell Culture

NIH 3T3 cells (mouse embryonic fibroblasts) obtained from Health Science Research Resources Bank (HSRRB; Osaka, Japan) were maintained in 75 cm^2 tissue culture flasks (TPP, Trasadingen, Switzerland) using DMEM with 10% fetal bovine serum (Sigma, MO, USA) and 1% antibiotic–antimycotic solution (Invitrogen, MD, USA) at 37°C under 5% CO_2 in a humidified incubator.

Assay of Cell Adhesion and Proliferation

Cultured NIH 3T3 cells were trypsinized and counted using a hemocytometer. NIH 3T3 cells were suspended in DMEM with 10% fetal bovine serum and 1% antibiotic–antimycotic solution at a concentration of 3×10^4 cells/mL. Before cell seeding, liquid atelocollagen solution was added to 96-well tissue culture plates (100 μL/well) and the plates were kept at 37°C to allow gelation. The cell suspension was added to SPG, AG, and a culture plate (100 μL/well). Thereafter, the cell cultures were maintained at 37°C under 5% CO_2 in a humidified incubator for 5 days. To estimate cell adhesion at day 1, 10 μL of tetrazolium solution (Cell Counting Kit-8; Dojin Glocal, Kumamoto, Japan) was added to each well of 96-well-culture plates after removal of the culture medium on SPG and AG. The plates were re-incubated at 37°C for 4 h. Absorbance was read at 490 nm with a spectrometer (ImmunoMini NJ-2300; System Instruments, Tokyo, Japan). This assay measures the amount of formazan produced in the reduction of the

tetrazolium by dehydrogenase in living cells, which is proportional to the number of living cells.

NIH 3T3 cells were also cultured on SPG, AG and the culture plate under the same conditions as those described above for 5 days. The culture medium was changed at days 1 and 3. Cell proliferation was estimated at days 1, 3, and 5 using tetrazolium solution.

Morphology of NIH3T3 cells was observed by a phase-contrast microscope (IX71; OLYMPUS, Tokyo, Japan) at days 1, 3, and 5.

Statistical Analysis

StatView for Windows (version 5.0) was used to determine means and standard deviation and for one-way analysis of variance (ANOVA). Fisher's PLSD method was used to compare differences among the means of cell number at day 1. Statistical significance was set at the level of $p = 0.05$.

RESULTS

Net Charge and Hydrogel Formation of Self-assembling Peptides

The net charges of peptides at different pH values are shown in Figure 1. The net charges of RADA16, KASEA16(+), and KASEA16(−) peptides under a neutral condition (pH 6–8) were 0, +2 and −2, respectively. Both KASEA16(+) and KASEA16(−) could form transparent hydrogels upon rapid neutralization using HEPES buffer without performing solvent substitution (Figure 2). Hydrogels were prepared from RADA16, KASEA16(+), and KASEA16(−) using the method involving solvent substitution. Under SEM observation, nanofibrous constituents of the RADA16, KASEA16(+), and KASEA16(−) hydrogels were uniform in width but still finer than those of AG (Figure 3). The diameters of nanofibers in the RADA16, KASEA16(+), and KASEA16(−) hydrogels and AG were 26.9 ± 4.1, 33.0 ± 4.4, 27.9 ± 5.1, and 48.1 ± 33.7 nm, respectively.

Evaluation of Cell Adhesion and Proliferation

The numbers of NIH3T3 cells that adhered to the KASEA16 (+) hydrogel, KASEA16(−) hydrogel, and AG at day 1 were significantly smaller than the number of cells that adhered to the conventional cell culture plate (Figure 4). The number of cells attached to the RADA16 hydrogel was comparable to that on the culture plate.

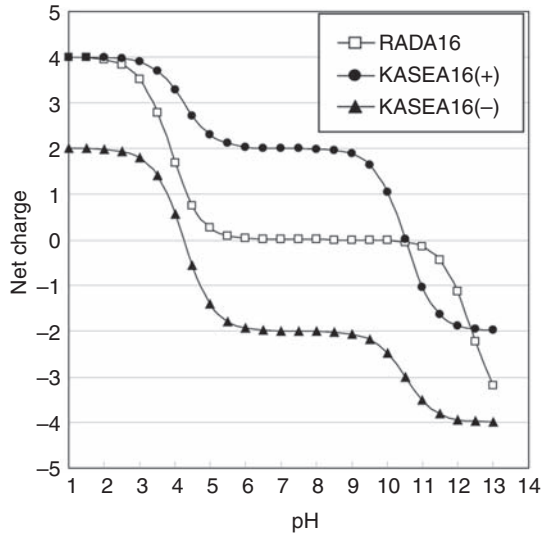

Figure 1. Net charge of self-assembling peptides at each pH.

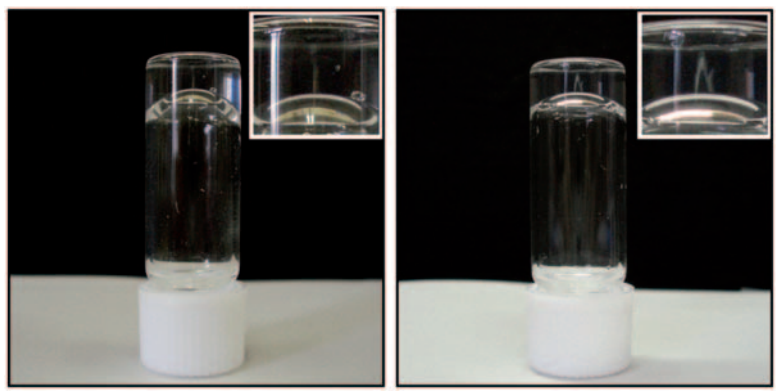

Figure 2. Formation of self-assembling peptide hydrogel. Transparent gels are formed when pH values of both solutions are adjusted to neutrality using HEPES buffer (pH 7.4).

NIH3T3 cells proliferated with time on all of the scaffolds in this study. Cells proliferated significantly on the RADA16 hydrogel as they did on the culture plates (Figure 5). Morphology and population of NIH3T3 cells differed depending on the scaffold (Figure 6). At day 1, NIH3T3 cells on the RADA16 hydrogel, KASEA16(+) hydrogel and culture plate showed extended cytoplasmic processes, while those on the

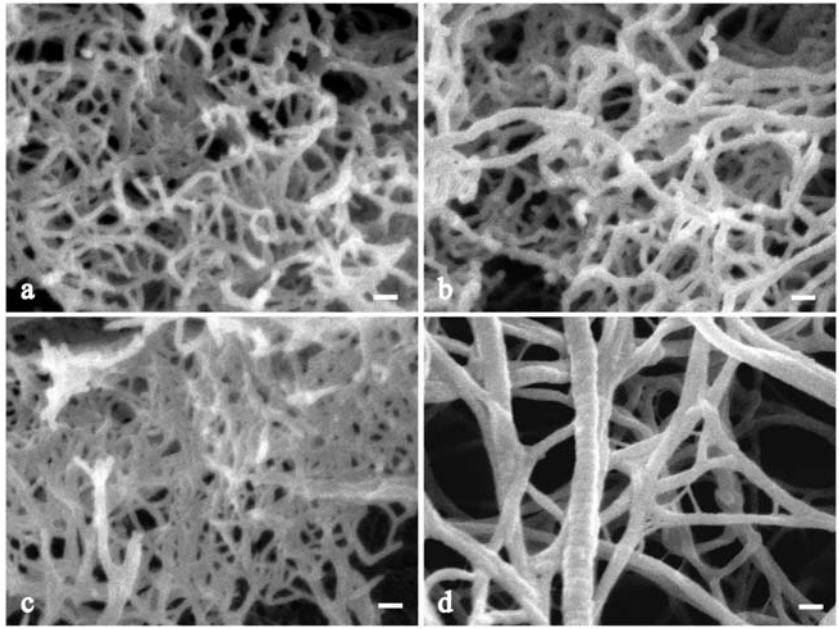

Figure 3. Comparsion by scanning electron microscopy of the nanofibers of RADA16 (a), KASEA16(+) (b), KASEA16(−) (c), and atelocollagen (d) gels. Fibers of atelocollagen gel are clearly thicker than those of the others. Bar = 100 nm.

KASEA16(−) hydrogel and AG were round shaped. Continuous cell growth was observed at days 3 and 5 on the RADA16 hydrogel, KASEA16(+) hydrogel, and culture plates. Cells on the KASEA16(+) hydrogel with spindle-like morphology increased in number, while cells on the RADA16 hydrogel and culture plates became round since the cells came into contact with each other towards confluency. On the KASEA16(−) hydrogel, the NHI3T3 cells formed clusters without extending cytoplasmic processes. In contrast, some cells with spindle-like shape on AG were observed at day 3, and a mixture of spindle-like cells and cell clusters was found at day 5.

DISCUSSION

In tissue engineering, safe and physically stable self-assembling peptides such as RADA16 ([CH_3CO]–RADARADARADARADA–[$CONH_2$]) have been examined as an alternative to scaffolding materials obtained from natural sources such as aletocollagen [23,26,30–32].

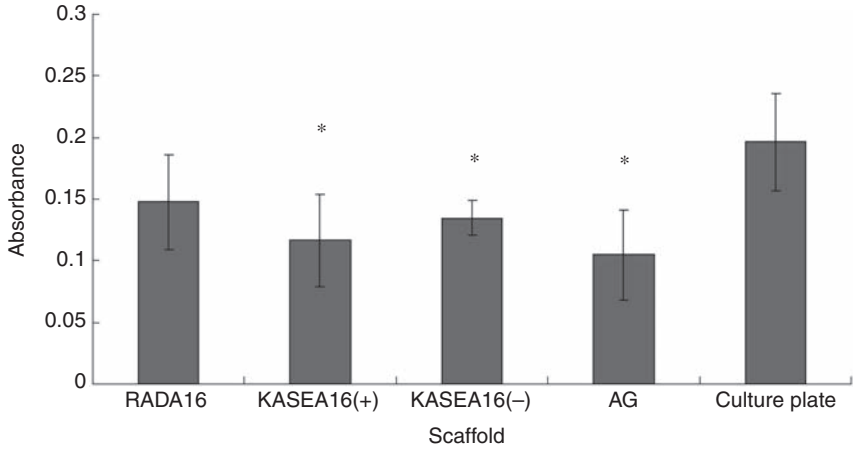

Figure 4. Comparison of NIH 3T3 cell adhesion at day 1 on different scaffolds. Number of cells, estimated from the absorbance of formazan, is largest in the culture plate. Values are presented as means ± SD. *Indicates a significant difference from the culture plate ($p < 0.05$).

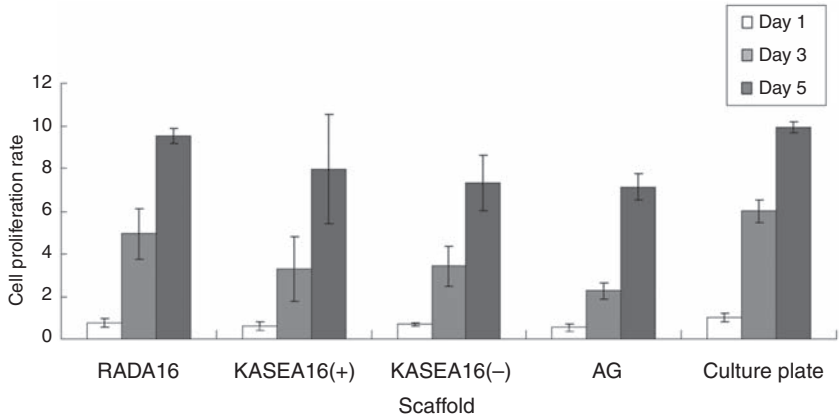

Figure 5. Comparison of NIH 3T3 cell proliferation at days 1, 3, and 5 on different scaffolds. Numbers of cells are estimated from the absorbance of formazan. Results are expressed as cell proliferation rate based on absorbance of the culture plate at day 1. NIH 3T3 cell proliferation rate increases over time. Values are means ± SD.

However, the RADA16 peptide tends to aggregate under a neutral condition due to strong electrostatic interactions between positively charged arginine residues and negatively charged aspartate residues [21,33]. Therefore, gradual neutralization by solvent substitution is required for forming a stable RADA16 hydrogel to use in cell culture.

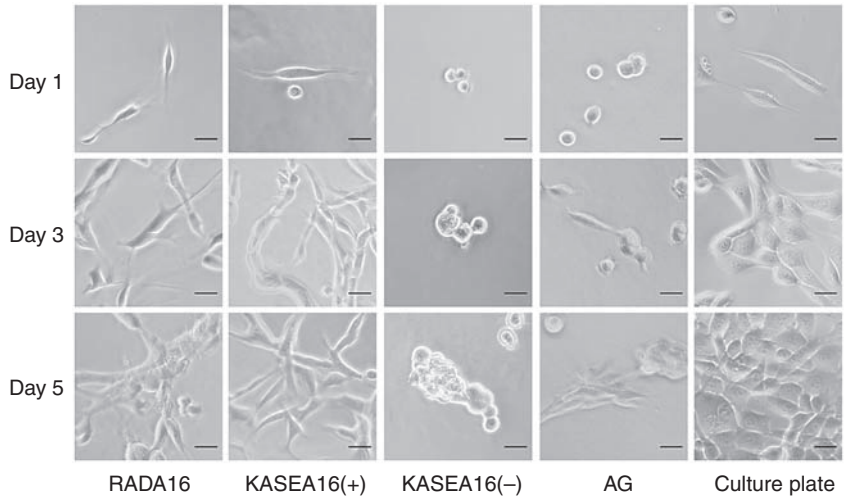

Figure 6. Morphological changes of NIH 3T3 cells on different scaffolds. NIH 3T3 cells with extended cytoplasmic processes are observed on RADA16 hydrogel, KASEA16(+) hydrogel and the culture plate at day 1. Cell density on these scaffolds becomes obvious at days 3 and 5. Cells on KASEA16(−) hydrogel are still round-shaped but later assembled to form cell clusters. Some cells with spindle-like shape on AG are observed at day 3, and a mixture of spindle-like cells and cell clusters are found at day 5. Bar = 50μm.

To overcome this problem, self-assembling peptides that form stable gels under a neutral condition are under evaluation [21,22,33,39]. In this study, we designed two new self-assembling peptides, KASEA16(+) ([CH_3CO]–KASAKAEAKAEAKASA–[$CONH_2$]) and KASEA16(−) ([CH_3CO]–SAEAKAEAKAEASAEA–[$CONH_2$]), the net charges of which are positive and negative, respectively, under a neutral condition. These peptides were shown to form hydrogels upon rapid pH neutralization without performing solvent substitution. The resulting hydrogels consisted of fine nanofibers with uniform width, as observed in the RADA16 hydrogel. A previous study showed that RATEA16 ([CH_3CO]–RATARAEARATARAEA–[$CONH_2$]) peptide, positively charged under a neutral condition, could form a stable hydrogel [21]. RATEA16 peptide is free from aggregation due to appropriate electrostatic interactions between arginine residues (positively charged) and glutamate residues (negatively charged), and it forms an antiparallel β-sheet structure and assembles into positively charged nanofibers. In addition, these nanofibers are distributed at appropriate distances and form a three-dimensional meshwork. As for the KASEA16(+) and

KASEA16(−) peptides, appropriate electrostatic interactions between positively charged lysine residues and negatively charged glutamate residues appear to prevent peptide aggregation under a neutral condition. The KASEA16(+) and KASEA16(−) peptides presumably form positively and negatively charged nanofibers, respectively. The appropriate electrostatic interactions among these charged nanofibers may contribute to the formation of a three-dimensional meshwork. Morphological structure of these gels clearly consists of three-dimensional meshwork as shown in previous studies [6,21]. Thus, the KASEA16(+) and KASEA16(−) peptides would be able to mix with cells in a neutral condition without aggregation and are expected to serve as scaffolds for three-dimensional cell culture.

Scaffolds have so far been evaluated by investigating morphology, attachment, and proliferation of cells cultured on scaffolds [22,40,41]. Chemical signals transmitted via cell surface receptors and physical signals such as scaffold stiffness affect cell functions, including morphology, proliferation, and differentiation [42–44]. The number and morphology of NIH3T3 cells attached to the RADA16 hydrogel were similar to those of cells attached to the cell culture plate. The numbers of cells attached to the KASEA16(+) hydrogel, KASEA16(−) hydrogel, and AG were similar, but cells with spindle-like morphology were observed only on the KASEA16(+) hydrogel. A stiff scaffold appeared to be a preferable scaffold for NIH3T3 cells to spread when it has the same surface structure as that of a soft scaffold [43,45,46]. Therefore, it is thought that the RADA16 hydrogel is probably the best scaffold for attachment of NIH3T3 cells, while the KASEA16(+) hydrogel provides a sufficiently rigid substrate for the cells to spread and attach. Even NIH3T3 cells could grow on all scaffolds in this study, but they became round and formed cell clusters on the KASEA16(−) gel. We therefore predict that electrostatic repulsions between the negatively charged nanofibers, which compose the KASEA16(−) hydrogel, and the negatively charged cell surface inhibit cells from extending their cytoplasmic processes and attaching to the hydrogel, finally resulting in the formation of cell clusters. It is noteworthy that NIH3T3 cells could spread better on the RADA16 and KASEA16(+) hydrogels than on AG, a proven scaffold material for cell culture. Furthermore, the cells on the RADA16 and KASEA16(+) hydrogels showed morphology and proliferation similar to those observed for cells on the culture plate. Consequently, since the KASEA16(+) peptide could form a stable hydrogel under a neutral condition, it is thought that the KASEA16(+) hydrogel will be a more useful scaffold than RADA16 hydrogel for cell culture.

CONCLUSIONS

In this study, we designed a new positively charged KASEA16(+) peptide and a new negatively charged KASEA16(−) peptide and evaluated their hydrogel formation ability. Comparison of these self-assembling peptides suggested that the charges of the scaffolds should be taken into consideration for the best design and selection of scaffolds for cell culture. The KASEA16(+) peptide could form a stable hydrogel under a neutral condition and the hydrogel served as a scaffold for cell proliferation.

ACKNOWLEDGMENTS

We are indebted to Dr. Yasuyuki Ishida at Chubu University for generously allowing us the use of a MALDI-TOF mass spectrometer.

REFERENCES

1. Drury, J.L. and Mooney, D.J. Hydrogels for Tissue Engineering: Scaffold Design Variables and Applications, *Biomaterials*, 2003: **24**: 4337–4351.
2. Hoffman, A.S. Hydrogels for Biomedical Applications, *Adv. Drug. Deliv. Rev.*, 2002: **54**: 3–12.
3. Fu, S., Guo, G., Gong, C. et al. Injectable Biodegradable Thermosensitive Hydrogel Composite for Orthopedic Tissue Engineering. 1. Preparation and Characterization of Nanohydroxyapatite/Poly(ethylene glycol)-Poly(epsilon-caprolactone)-Poly(ethylene glycol) Hydrogel Nanocomposites, *J. Phys. Chem. B*, 2009: **113**: 16518–16525.
4. Ozeki, M., Kuroda, S., Kon, K. and Kasugai, S. Differentiation of Bone Marrow Stromal Cells into Osteoblasts in a Self-assembling Peptide Hydrogel: In Vitro and In Vivo Studies, *J. Biomater. Appl.*, 2010 (Epub ahead of print).
5. Ramachandran, S., Tseng, Y. and Yu, Y.B. Repeated Rapid Shear-Responsiveness of Peptide Hydrogels with Tunable Shear Modulus, *Biomacromolecules*, 2005: **6**: 1316–1321.
6. Takei, J. Self-assembling 3-Dimensional Scaffold Peptide Hydrogel for Bone Regeneration, *J. Jpn. Assoc. Regenerative Dent.*, 2005: **3**: 1–11.
7. Zhang, S., Gelain, F. and Zhao, X. Designer Self-assembling Peptide Nanofiber Scaffolds for 3D Tissue Cell Cultures, *Semin. Cancer. Biol.*, 2005: **15**: 413–420.
8. Ichioka, S., Ohura, N., Sekiya, N., Shibata, M. and Nakatsuka, T. Regenerative Surgery for Sacral Pressure Ulcers Using Collagen Matrix Substitute Dermis (Artificial Dermis), *Ann. Plast. Surg.*, 2003: **51**: 383–389.
9. Yamada, N., Uchinuma, E. and Kuroyanagi, Y. Clinical Evaluation of an Allogeneic Cultured Dermal Substitute Composed of Fibroblasts Within a Spongy Collagen Matrix, *Scand. J. Plast. Reconstr. Surg. Hand Surg.*, 1999: **33**: 147–154.

10. Knapp, T.R., Kaplan, E.N. and Daniels, J.R. Injectable Collagen for Soft Tissue Augmentation, *Plast. Reconstr. Surg.*, 1977: **60**: 398–405.
11. Kojima, K. and Amano, T. Injectable Collagen for Soft Tissue Contour Defects, *J. Transportation Med.*, 1985: **39**: 6–13.
12. Ono, I., Zhou, L.J. and Tateshita, T. Effects of a Collagen Matrix Containing Prostaglandin E(1) on Wound Contraction, *J. Dermatol. Sci.*, 2001: **25**: 106–115.
13. Ono, I., Tateshita, T. and Inoue, M. Effects of a Collagen Matrix Containing Basic Fibroblast Growth Factor on Wound Contraction, *J. Biomed. Mater. Res.*, 1999: **48**: 621–630.
14. Charriere, G., Bejot, M., Schnitzler, L., Ville, G. and Hartmann, D.J. Reactions to a Bovine Collagen Implant. Clinical and Immunologic Study in 705 Patients, *J. Am. Acad. Dermatol.*, 1989: **21**: 1203–1208.
15. Katsube, K., Ochi, M., Uchio, Y. et al. Repair of Articular Cartilage Defects with Cultured Chondrocytes in Atelocollagen Gel. Comparison with Cultured Chondrocytes in Suspension, *Arch. Orthop. Trauma Surg.*, 2000: **120**: 121–127.
16. Uchio, Y., Ochi, M., Matsusaki, M., Kurioka, H. and Katsube, K. Human Chondrocyte Proliferation and Matrix Synthesis Cultured in Atelocollagen Gel, *J. Biomed. Mater. Res.*, 2000: **50**: 138–143.
17. Ito, Y., Ochi, M., Adachi, N. et al. Repair of Osteochondral Defect with Tissue-engineered Chondral Plug in a Rabbit Model, *Arthroscopy*, 2005: **21**: 1155–1163.
18. Nagayasu, A., Hosaka, Y., Yamasaki, A. et al. A Preliminary Study of Direct Application of Atelocollagen into a Wound Lesion in the Dog Cornea, *Curr. Eye Res.*, 2008: **33**: 727–735.
19. Zhang, S., Holmes, T., Lockshin, C. and Rich, A. Spontaneous Assembly of a Self-complementary Oligopeptide to Form a Stable Macroscopic Membrane, *Proc. Natl. Acad. Sci. USA*, 1993: **90**: 3334–3338.
20. Zhang, S., Lockshin, C., Cook, R. and Rich, A. Unusually Stable Beta-sheet Formation in an Ionic Self-complementary Oligopeptide, *Biopolymers*, 1994: **34**: 663–672.
21. Zhao, Y., Yokoi, H., Tanaka, M., Kinoshita, T. and Tan, T. Self-assembled pH-responsive Hydrogels Composed of the RATEA16 Peptide, *Biomacromolecules*, 2008: **9**: 1511–1518.
22. Kretsinger, J.K., Haines, L.A., Ozbas, B., Pochan, D.J. and Schneider, J.P. Cytocompatibility of Self-assembled Beta-hairpin Peptide Hydrogel Surfaces, *Biomaterials*, 2005: **26**: 5177–5186.
23. Horii, A., Wang, X., Gelain, F. and Zhang, S. Biological Designer Self-assembling Peptide Nanofiber Scaffolds Significantly Enhance Osteoblast Proliferation, Differentiation and 3-D Migration, *PLoS One*, 2007: **2**: 1–9.
24. Zhang, S., Lockshin, C., Herbert, A., Winter, E. and Rich, A. Zuotin, a Putative Z-DNA Binding Protein in Saccharomyces Cerevisiae, *EMBO J.*, 1992: **11**: 3787–3796.
25. Zhang, S., Holmes, T.C., DiPersio, C.M., Hynes, R.O., Su, X. and Rich, A. Self-complementary Oligopeptide Matrices Support Mammalian Cell Attachment, *Biomaterials*, 1995: **16**: 1385–1393.

26. Holmes, T.C., de Lacalle, S., Su, X., Liu, G., Rich, A. and Zhang, S. Extensive Neurite Outgrowth and Active Synapse Formation on Self-assembling Peptide Scaffolds, *Proc. Natl. Acad. Sci. USA*, 2000: **97**: 6728–6733.
27. Caplan, M.R., Moore, P.N., Zhang, S., Kamm, R.D. and Lauffenburger, D.A. Self-assembly of a Beta-sheet Protein Governed by Relief of Electrostatic Repulsion Relative to van der Waals Attraction, *Biomacromolecules*, 2000: **1**: 627–631.
28. Kisiday, J., Jin, M., Kurz, B. et al. Self-assembling Peptide Hydrogel Fosters Chondrocyte Extracellular Matrix Production and Cell Division: Implications for Cartilage Tissue Repair, *Proc. Natl. Acad. Sci. USA*, 2002: **99**: 9996–10001.
29. Jun, S., Hong, Y., Imamura, H., Ha, B.Y., Bechhoefer, J. and Chen, P. Self-assembly of the Ionic Peptide EAK16: The effect of Charge Distributions on Self-assembly, *Biophys. J.*, 2004: **87**: 1249–1259.
30. Semino, C.E., Merok, J.R., Crane, G.G., Panagiotakos, G. and Zhang, S. Functional Differentiation of Hepatocyte-like Spheroid Structures from Putative Liver Progenitor Cells in Three-dimensional Peptide Scaffolds, *Differentiation*, 2003: **71**: 262–270.
31. Degano, I.R., Quintana, L., Vilalta, M. et al. The Effect of Self-assembling Peptide Nanofiber Scaffolds on Mouse Embryonic Fibroblast Implantation and Proliferation, *Biomaterials*, 2009: **30**: 1156–1165.
32. Davis, M.E., Motion, J.P., Narmoneva, D.A. et al. Injectable Self-assembling Peptide Nanofibers Create Intramyocardial Microenvironments for Endothelial Cells, *Circulation*, 2005: **111**: 442–450.
33. Yokoi, H. and Kinoshita, T. (2008). Design of Self-assembling Peptides to Form Transparent Gels at Neutral pH, In: Aimoto, S. and Ono, S. (eds), *Peptide Science* 2007, Osaka, The Japanese Peptide Society, pp. 109–110.
34. Ye, Z., Zhang, H., Luo, H. et al. Temperature and pH Effects on Biophysical and Morphological Properties of Self-assembling Peptide RADA16-I, *J. Pept. Sci.*, 2008: **14**: 152–162.
35. Genove, E., Shen, C., Zhang, S. and Semino, C.E. The Effect of Functionalized Self-assembling Peptide Scaffolds on Human Aortic Endothelial Cell Function, *Biomaterials*, 2005: **26**: 3341–3351.
36. Guo, J., Su, H., Zeng, Y. et al. Reknitting the Injured Spinal Cord by Self-assembling Peptide Nanofiber Scaffold, *Nanomedicine*, 2007: **3**: 311–321.
37. Lehninger, A.L. (1979). *Biochimie*, 2nd edn, Paris, Flarnmarion.
38. Inoue, T. and Osatake, H. A New Drying Method of Biological Specimens for Scanning Electron Microscopy: The t-Butyl Alcohol Freeze-drying Method, *Arch. Histol. Cytol.*, 1988: **51**: 53–59.
39. Aggeli, A., Bell, M., Boden, N., Carrick, L.M. and Strong, A.E. Self-assembling Peptide Polyelectrolyte Beta-sheet Complexes Form Nematic Hydrogels, *Angew. Chem. Int. Ed. Engl.*, 2003: **42**: 5603–5606.
40. Gelain, F., Lomander, A., Vescovi, A.L. and Zhang, S. Systematic Studies of a Self-assembling Peptide Nanofiber Scaffold with Other Scaffolds, *J. Nanosci. Nanotechnol.*, 2007: **7**: 424–434.
41. Bacakova, L., Filova, E., Rypacek, F., Svorcik, V. and Stary, V. Cell Adhesion on Artificial Materials for Tissue Engineering, *Physiol. Res.*, 2004: **53**: S35–45.

42. Genes, N.G., Rowley, J.A., Mooney, D.J. and Bonassar, L.J. Effect of Substrate Mechanics on Chondrocyte Adhesion to Modified Alginate Surfaces, *Arch. Biochem. Biophys.*, 2004: **422**: 161–167.
43. Yeung, T., Georges, P.C., Flanagan, L.A. et al. Effects of Substrate Stiffness on Cell Morphology, Cytoskeletal Structure, and Adhesion, *Cell Motil. Cytoskeleton*, 2005: **60**: 24–34.
44. Flanagan, L.A., Ju, Y.E., Marg, B., Osterfield, M. and Janmey, P.A. Neurite Branching on Deformable Substrates, *Neuroreport*, 2002: **13**: 2411–2415.
45. Lo, C.M., Wang, H.B., Dembo, M. and Wang, Y.L. Cell Movement is Guided by the Rigidity of the Substrate, *Biophys. J.*, 2000: **79**: 144–152.
46. Wang, H.B., Dembo, M. and Wang, Y.L. Substrate Flexibility Regulates Growth and Apoptosis of Normal But Not Transformed Cells, *Am. J. Physiol. Cell Physiol.*, 2000: **279**: C1345–1350.